Available online at www.sciencedirect.com

ScienceDirect

Procedia Engineering 2 (2010) 1605–1616

Procedia Engineering

www.elsevier.com/locate/procedia

Fatigue 2010

Assessment of Improvement Techniques Effect on Fatigue Behaviour of Friction Stir Welded Aerospace Aluminium Alloys

Catarina Vidal, Virgínia Infante[a]*, Pedro Vilaça[a]

[a]*Instituto Superior Técnico, Av. Rovisco Pais, 1096-001 Lisboa, Portugal*

Recieved 10 February 2010; revised 9 March 2010; accepted 15 March 2010

Abstract

This research work is based on analysis of the improvement of friction stir welded joints of the aerospace aluminium alloy AA2024-T351. Therefore, initially, the Taguchi method was used to obtain the optimal FSW parameters for improvement its mechanical behaviour. Then the fatigue resistance of base material, joints in as-welded condition and sound and defective FSW welded joints improved by grinding were detailed investigated. The influence of process parameters was addressed via statistical analysis of weld bead appearance parameters, mechanical tensile and bending resistance, metallurgical features and hardness field characterization. Validation tests demonstrate the Taguchi design's feasibility in the optimization of the FSW parameters and fatigue results show the resistance of improved welded joints overcoming base material.

Keywords: Friction Stir Welding, AA2024-T351, Taguchi Method, Grinding, Fatigue

1. Introduction

Aluminum alloys market for aeronautic and aerospace industries is still expanding due to their unique characteristics 0. Furthermore, the nature of welding in the aeronautic industry is characterized by low unit production, high unit cost, extreme reliability, and severe service conditions. Nevertheless, welding in the aeronautics industry is experiencing exciting developments [1].

Friction Stir Welding (FSW) is perhaps the most remarkable and potentially useful new welding technique to be introduced in the recent past [2], [3]. FSW is a purely mechanical process and because it takes place in the solid phase, all the problems related to the solidification of a melted material are avoided [4], [5]. Some aeronautic companies are already applying FSW in their products and services [6], [7], [8].

Thermal efficiency of FSW is above 90% [9], and allows complete recycling of the welded structure in opposition to other joining technologies also applied to aluminum alloys in aircrafts as adhesives.

Fatigue is undoubtedly the major design criterion in aeronautic structures [10], [11]. Nevertheless, in the literature, comprehensive design data including tensile, fatigue, fracture toughness and fatigue crack propagation were generally not reported together for welds in aeronautic aluminium alloy series.

Although the typical quality assurance of FSW seams some defects may occur, mainly in conventional FSW, such as root defects, e.g., lack of penetration and/or particles alignment [12]. These defects along with the relatively

* Corresponding author. Tel.: +351 218417643.
E-mail address: virginia@dem.ist.utl.pt.

1877-7058
doi:10.1016/j.proeng.2010.03.173

low residual stresses of the FSW thermo-mechanical cycle can turn into primary sources of crack initiation. Also, geometrical sharp changes, such as, the ones eventually resulted from interaction between components top surface and the FSW tool shoulder can reduce fatigue life. Recognising that some of these defects might occur, leading to the development of a number of improvement techniques for increasing the fatigue life of the welded joints [13], [14], [15]. This has instigated the need for feasible techniques and methods that enable the remove of a thin superficial layer at the vicinity of the root of the weld seam and alleviate the residual stresses in welded components.

In this context, this paper deals with the fatigue behaviour of FSW joints subjected to surface smoothing by grinding improvement technique. The reason for selection of this procedure is to overcome eventual burr at specimen's top surface and root defects. Moreover, grinding is a low-cost and relatively easy to automate procedure becoming nowadays an accepted industrial post-FSW procedure for the most fatigue resistance demanding applications, e.g., aeronautic. In this work, the Taguchi method was used to obtain the optimal FSW parameters for improvement mechanical behaviour of the 2024-T351 aluminium alloy.

The paper starts with the introduction of the plan of experiments with the selection of the welding performance and FSW parameters and their levels. The base material (BM), FSW procedures, improvement technique features including visual appearance of "as-welded" and ground conditions were also presented. The obtained results such as macro and micrographs and hardness profile of the FSW joints in "as-welded" condition, mechanical efficiency of the welded specimens under tensile and bending static load were analysed and discussed. Other tests were also conducted, such as fatigue test for BM and FSW joints in different conditions. Fractographic analysis of the FSW joints are also presented and analysed.

2. Plan of Experiments

The experimental tests were planned using Taguchi method. Taguchi proposed an experimental plan in terms of orthogonal array that gives different combinations of parameters and their levels for each experiment [16]. Knowing the contribution of individual parameters is the key to deciding the nature of the control to be established on a production process. Analysis of variance (ANOVA) is a statistical treatment most commonly applied to the results of the experiments to determine the percentage contribution of each parameter against a stated level of confidence.

In the standard approach, the results of a single run or the average of repetitive runs are processed through the main effect and ANOVA (raw data analysis). The second approach, which Taguchi strongly recommends for multiple runs, is to use the signal-to-noise (S/N) ratio for the same steps in the analysis. In the present investigation, only the raw data analysis was performed. The effects of the selected FSW parameters on the selected performance characteristics were investigated through the plots of the main effects based on raw data. An algebraic model for predicting the best mechanical performance was also developed. Experiments were conducted to support the optimal FSW parameters.

2.1. Welding performance assessment

In order to assess the quality of the welded joint relatively to the base material properties, a coefficient called Global Efficiency to Tensile Strength, GETS (1) was developed by Vilaça [9]:

$$GETS = C_E \frac{E_i}{E_{BM}} + C_{\sigma y} \frac{\sigma_{y_i}}{\sigma_{y_{BM}}} + C_{\sigma UTS} \frac{\sigma_{UTS_i}}{\sigma_{UTS_{BM}}} + C_A \frac{A_i}{A_{BM}} + C_{UT} \frac{UT_i}{UT_{BM}} \quad (1)$$

In analogy with the tensile tests and the GETS coefficient, a Global Efficiency to Bending, GEB (2) was also considered:

$$GEB = C_F \frac{F_i}{F_{BM}} + C_d \frac{d_i}{d_{BM}} + C_{UB} \frac{UB_i}{UB_{BM}} \quad (2)$$

Where: E is the Young modulus; σy and σUTS, the yield and ultimate stress, respectively; A, elongation; UT, toughness; F, maximum load; d, displacement at maximum load and UB is the energy consumed until a minimum specified load is reached.

The weights considered in (1) and (2) are shown in Table 1. These weights aim at consider the relative importance level of the mechanical properties in design of aeronautic structures.

Table 1. Weights considered for GETS and GEB

GETS		GEB	
C_{σ_y}	0.30		
$C_{\sigma_{UTS}}$	0.25	C_{U_B}	0.50
C_A	0.20	C_F	0.25
C_{U_T}	0.20	Cd	0.25
C_E	0.05		

Because the hardness results are important in assessing the relative mechanical properties between the different zones resulting from the thermo-mechanical FSW cycle it was established the following expression (3) as a welding performance parameter:

$$HARD = \frac{Minimum\ hardness}{BM\ hardness} \quad (3)$$

where HARD means HArdness Ration Drop, *minimum hardness* is the lowest hardness value measured at the mid-thickness of the cross section of the weld seam and *BM hardness* is the base metal hardness value.

2.2. Selection of FS welding parameters and their levels

In order to obtain welds without defects, with high fatigue resistance, three FSW parameters were chosen, namely vertical downward forging force, travel speed and pin length. These three parameters together allow control the defect that is more difficult to eliminate in sound welds, i.e. lack of penetration and/or particles alignment in the root. The choice of the number of levels and their values were based on preliminary experimental tests. Analyzed the samples produced, three levels for each parameter were selected whose values are presented in Table 2:

2.3. Orthogonal array experiment

To select an appropriate orthogonal array for experiments, the total degrees of freedom need to be computed. The degrees of freedom are defined as the number of comparisons between process parameters that need to be made to determine which level is better and specifically how much better it is [17]. In the present study, the interaction between the welding parameters is neglected. Therefore, there are six degrees of freedom owing to the three welding parameters. Once the degrees of freedom required are known, the next step is to select an appropriate orthogonal array to fit the specific task. In this study, an L9 orthogonal array was used. Each FS welding parameter is assigned to a column and twenty seven welding parameter combinations are available. A total of nine experimental runs must be conducted, using the combination of levels for each control factor (A–D) as indicated in Table 3.

Table 2. Friction stir welding parameters and their levels

FSW parameter	Symbol	Level 1	Level 2	Level 3
Variable parameters				
Vertical force (kg)	A	850	900	950
Travel speed (mm/min)	B	120	250	500
Pin length (mm)	C	4.00	4.08	4.17
Constant parameters				
Tilt angle		0°		
Rotation speed		1000 rpm		
Rotation direction		CW		
Plunge speed		0.1 mm/s		
Dwell time		8 s		
FSW control		Vertical force control		

However, this study did not use all the array cells for four factors, because only three factors were considered (vertical downward forging force, travel speed and pin length). Therefore, the last column (for the fourth factor) in the L_9 orthogonal array is left empty for this specific study.

The selected parameters, as discussed in *Section 2.2*, are listed in Table 2 along with their applicable codes and values for use in the Taguchi parameter design study.

Table 3. The basic Taguchi $L_9(3^4)$ orthogonal array

Run	Control factors and levels			
	A	B	C	D
1	1	1	1	1
2	1	2	2	2
3	1	3	3	3
4	2	1	2	3
5	2	2	3	1
6	2	3	1	2
7	3	1	3	2
8	3	2	1	3
9	3	3	2	1

3. Experimental set-up and Results

3.1. Base material and FSW procedure

The 2024-T351 aluminium alloy was used in this investigation for being one of the most popular materials in aeronautic applications. Chemical composition and mechanical properties of this alloy are presented in Tables 4 and 5, respectively. All the welds were performed in plates rolled to 4 mm thick perpendicular to the rolling direction in a butt joint arrangement with straight edge preparation. Plates of 200 mm x 145(RD) mm were welded along the length. The FSW equipment used was an ESAB Legio FSW 3UL. Plunge and dwell periods (vx=0) were performed under vertical position control and weld period (vx>0) was carry out under vertical downward force control. The FSW tool that was use to perform all the welds is a patented modular concept of FSW tools. This tool is based on 3 main components: Body; Shoulder and Pin, which enable the easy replacement of any damage component and the combination between different shoulder and pin geometries (Fig. 1). Moreover, this tool enables internal forced refrigeration and the setting of any length for the pin. The pin is 9º conical with a bottom diameter of 4 mm and LH threads along his length. The shoulder is plane with 2 spiral striates scrolling an angle of 180º with outer and inner diameter of 16 mm and 5 mm, respectively. The FSW parameters implemented are shown in Table 2.

Table 4. Chemical composition of 2024-T351 aluminium alloy, % weight

Al	Mg	Cu	Mn
89.87	3.38	6.20	0.55

Fig. 1. Modular tool used during FSW trials

Table 5. Mechanical properties of 2024-T351 aluminium alloy

Young modulus (GPa)	Yield stress (MPa)	Ultimate stress (MPa)	Elongation (%)	Toughness (J/mm^3)
75.5	383.8	533.8	22.0	80.7

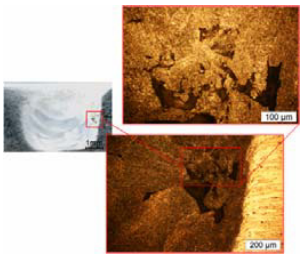

Fig. 2. Optical macro and micrograph of the FSW seam of experiment 3 showing voids in the advancing side

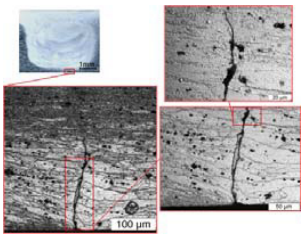

Fig. 3. Optical macro and micrograph of the FSW seam of experiment 6 showing lack of penetration, typically addressed as kissing bond

3.2. Metallographic characterization

For the metallographic characterization the samples are mounted, polished down to 1 µm and etched with Keller reagent. Then the different metallurgical zones are identified for detailed micrograph analysis. The macro and micrographs of some defective welded seams can be observed in Figures 2 and 3

3.3. Hardness measurements

The hardness field was established in the cross section of the weld seams according to the ISO 6507-2 with 0.5 kg and about 28 measured points on the middle surface (mid-thickness).

Table 6 shows the results obtained for HARD coefficient.

3.4. Mechanical properties under static loading

Both uniaxial tensile and bending tests were performed on an Instron 1342, with a load cell of 250kN and high resolution biaxial extensometers. Specimens were taken from each welded plate for tensile tests, with geometry according to the EN-895-2002. Bending tests of 90º were also carried out. The average distance between supports (distance between the centres of support rolls) is 30 mm. Support rolls diameter is 10 mm and mandrel radius is 5 mm. The mandrel velocity used throughout the trial was 1 mm/min. From each welded condition two specimens were taken and bended with the root of the weld seam under tensile stress. All mechanical trials were performed at room temperature. Table 5 summarizes all the mechanical properties assessed for the base material and

Table 6 shows the results obtained for GETS and GEB for FSW specimens in “as-welded” condition.

3.5. Computation of average performance

The experimental data was analyzed and the optimal levels for all the control factors were identified. The results of GETS, GEB and HARD of each sample are shown in

Table 6. There are three categories of performance characteristics, i.e., the lower-the-better, the higher-the-better, and the nominal-the-better. To improve the mechanical behaviour of AA2024-T351, the higher-the-better performance characteristic for GETS, GEB and HARD should be taken for obtaining optimal welding performance.

Table 6. Experimental results

Experiment Number	FSW parameter Level			GETS	GEB	HARD
	A	B	C			
1	850	120	4.00	0.5847	0.5176	0.6564
2	850	250	4.08	0.6269	0.3617	0.7730
3	850	500	4.17	0.5978	0.4698	0.7362
4	900	120	4.08	0.5851	0.6289	0.7423
5	900	250	4.17	0.6853	0.5922	0.7791
6	900	500	4.00	0.5302	0.2773	0.8712
7	950	120	4.17	0.5850	0.5060	0.7116
8	950	250	4.00	0.5549	0.3289	0.7546
9	950	500	4.08	0.5763	0.3179	0.7975

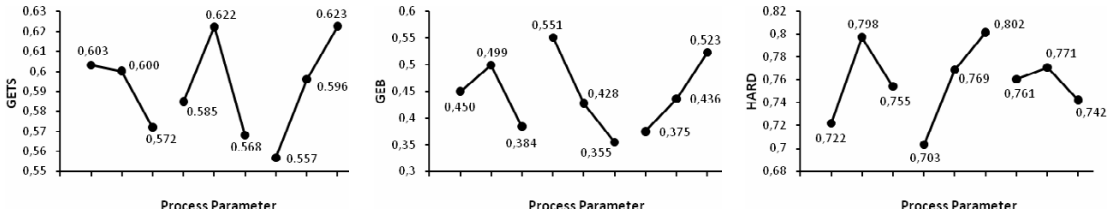

Fig. 4. Effect of process parameters on GETS, GEB and HARD coefficients, respectively

All three levels of every factor are equally represented in 9 experiments. Since the experimental design is orthogonal, it is possible to separate the effect of each factor at each level [18]. The average of quality characteristic for each parameter is the mean response at each level. For example, the mean percentage GETS for travel speed at level 1 can be calculated by averaging GETS from the experiments 1, 4 and 7. GETS, GEB and HARD for each parameter at each level were calculated. These are also called as main effects. Fig. 4 shows the GETS, GEB and HARD response (main effects), respectively.

3.6. Analysis of variance (ANOVA)

The information about how significant the effect of each controlled parameter is on the quality characteristic of interest can be obtained. ANOVAs for raw data has been performed to identify the significant parameters and to quantify their effect on the performance characteristic. The ANOVA based on the raw data identifies the factors which affect the average response rather than reducing variation [16]. Tables 7-9 show the results of ANOVA for GETS, GEB and HARD, respectively.

Table 7. Results of the analysis of variance for GETS

Source	DOF	Sum of squares	Mean square	F ratio	Contribution (%)
A	2	0.00176	0.00088	0.7014	11.35
B	2	0.00463	0.00231	1.8415	29.79
C	2	0.00663	0.00331	2.6385	42.68
Error	2	0.00251	0.00126		16.18
Total	8	0.01553			100

Table 8. Results of the analysis of variance for GEB

Source	DOF	Sum of squares	Mean square	F ratio	Contribution (%)
A	2	0.02003	0.01001	1.1274	15.43
B	2	0.05880	0.02940	3.3104	45.31
C	2	0.03318	0.01659	1.8680	25.57
Error	2	0.01776	0.00888		13.69
Total	8	0.12977			100

Table 9. Results of the analysis of variance for HARD

Source	DOF	Sum of squares	Mean square	F ratio	Contribution (%)
A	2	0.00864	0.00432	2.5825	30.60
B	2	0.01499	0.00749	4.4800	53.08
C	2	0.00126	0.00063	0.3775	4.47
Error	2	0.00335	0.00167		11.85
Total	8	0.02824			100

3.7. Algebraic model for optimum parameters

In order to improve the fatigue behaviour of the FSW joints, which is the main goal of this work, and because three different parametric combinations were obtained, one for each welding parameter performance (Fig. 4), an algebraic model (4) was developed considering the percentage contribution of each process parameter (Table 10).

Table 10. Percentages contribution

	Force		Travel Speed		Pin Length	
GETS	$\rho_{A_{GETS}}$	11.35	$\rho_{B_{GETS}}$	29.79	$\rho_{C_{GETS}}$	42.68
GEB	$\rho_{A_{GEB}}$	15.43	$\rho_{B_{GEB}}$	45.31	$\rho_{C_{GEB}}$	25.57
HARD	$\rho_{A_{HARD}}$	30.60	$\rho_{B_{HARD}}$	53.08	$\rho_{C_{HARD}}$	4.47
TOTAL	ρ_{A_T}	57.38	ρ_{B_T}	128.18	ρ_{C_T}	72.72

$$\begin{bmatrix} Force & x & x \\ x & Speed & x \\ x & x & Pin \end{bmatrix} = \begin{bmatrix} A_1 & A_2 & A_2 \\ B_2 & B_1 & B_3 \\ C_3 & C_3 & C_2 \end{bmatrix} \begin{bmatrix} \frac{\rho A_{GETS}}{\rho A_T} & \frac{\rho B_{GETS}}{\rho B_T} & \frac{\rho C_{GETS}}{\rho C_T} \\ \frac{\rho A_{GEB}}{\rho A_T} & \frac{\rho B_{GEB}}{\rho B_T} & \frac{\rho C_{GEB}}{\rho C_T} \\ \frac{\rho A_{HARD}}{\rho A_T} & \frac{\rho B_{HARD}}{\rho B_T} & \frac{\rho C_{HARD}}{\rho C_T} \end{bmatrix} \quad (4)$$

Each column of the first matrix on the right side corresponds to the parametric optimal combination found, respectively, for GETS, GEB and HARD.

$$\begin{bmatrix} Force & x & x \\ x & Speed & x \\ x & x & Pin \end{bmatrix} = \begin{bmatrix} 850 & 900 & 900 \\ 250 & 120 & 500 \\ 4.17 & 4.17 & 4.08 \end{bmatrix} \begin{bmatrix} 0.1978 & 0.2324 & 0.5869 \\ 0.2690 & 0.3535 & 0.3516 \\ 0.5333 & 0.4141 & 0.0615 \end{bmatrix}$$

It was obtained the following parametric combination:

Force = 168.13 + 242.10 + 479,97 = 890kg ; Speed = 58.1 + 42.42 + 207.05 = 308mm / min ; Pin = 2.45 + 1.47 + 0.25 = 4.17mm

This combination will be considered the optimal FSW combination.

3.8. Confirmation test

Once the optimal level of the process parameters is selected, the final step is to verify the improvement of the performance characteristics using the optimal level of the process parameters. Therefore, further experimental tests were carried out to validate the developed algebraic model. The macro and micrographs of the welded plates can be observed in Fig. 5. The hardness field established in the cross section of the weld seam with 0.5 kg and about 53 measured points along 3 representative penetration levels: 0.5mm from top surface (top level); mid-thickness (middle level); 0.5mm from bottom surface (bottom level) can be observed in Fig. 6. Table 10 shows the results of the confirmation experiment for GETS and GEB.

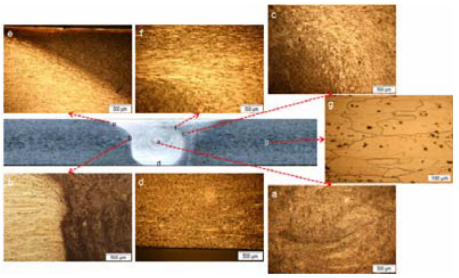

Fig. 5. Metallographic results

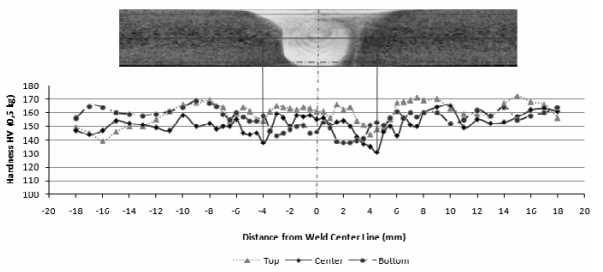

Fig. 6. Hardness profiles at 3 different levels (top, middle and bottom) of the cross section of the FSW seam

Table 11. Results of the confirmation experiment

	Optimal FS welding parameters		
	Prediction for GETS	Prediction for GEB	Experiment
Level	$A_1B_2C_3$	$A_2B_1C_3$	$A_{EM}B_{EM}C_{EM}$
GETS value	66.4 %		71.3 %
GEB value		68.4 %	69.2 %

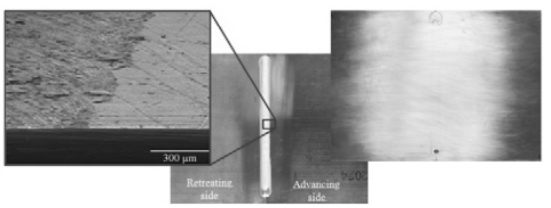

Fig. 7. View of the top surface of the FS welded specimens. "as-welded" condition (center); detail of burr in advancing side (left); ground condition (right).

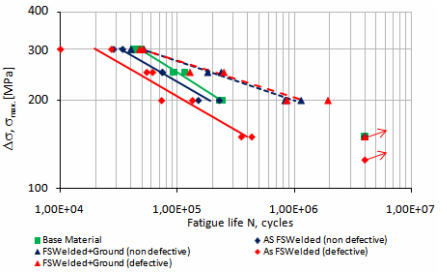

Fig. 8. *S-N* curves (R=0) for base material and FSW specimens in conditions: "as-welded*"* and post weld smoothed surface by grinding.

3.9. Application of the improvement technique

After welding, an improvement technique was applied at both top and bottom surfaces of the plates. The improvement technique selected was the grinding procedure resulting in a post-FSW smoothed surface condition. The grinding procedure by surface polishing resulted in a superficial mean roughness of 0.5 µm. The layer extracted at each surface was about 50 µm. It is presented in Fig. 7, photographs of top surface of welded specimens, before and after the application of the selected improvement technique.

3.10. Fatigue testing data

The specimens were fatigue tested under sinusoidal axial tensile constant amplitude loading performed on an Instron 1342, with a load cell of 250 kN. Stress ratio was set to R=0 and the oscillation frequency 11-15Hz. The *S-N* curve results obtained are presented in Fig. 8. The specimens were tested to complete failure, or to an endurance of 4 million cycles if there was no evidence of fatigue cracking. The fracture surfaces of the FSW specimens "as-welded" and ground were analysed at macro and micro level with SEM. The observations obtained are presented in

Figures 9 and 10. In both illustrated cases, FSW "as-welded" condition and ground condition, the fracture occurred at the retreating side starting at the top surface in the vicinity of the residual burr (see Fig. 7).

4. Analysis of the Results

4.1. Fatigue testing data

Some of the most relevant metallurgical aspects of the FSW joints produced are identified in the micrographs of Fig. 5. These metallurgical features are well known intrinsic characteristics of the typical zones identified in the macrograph of Fig. 11, namely the base material (BM), heat affected zone (HAZ), thermomechanically affected zone (TMAZ) and dynamically recovered zone (nugget).

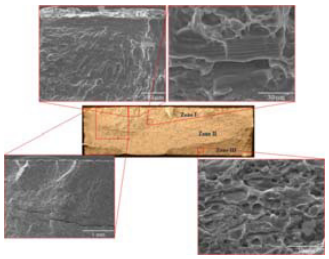

Fig. 9. Fracture surface resultant from fatigue trial of sounds FSW specimens in the "as-welded" condition (stress range=300 MPa)

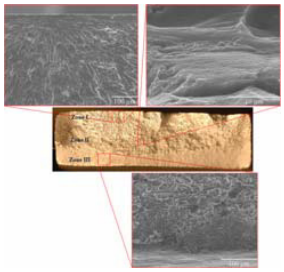

Fig. 10. Fracture surface resultant from fatigue trial of sound FSW specimens in the ground surfaces condition (stress range=300 MPa)

The nugget (detail "a" in Fig. 5) presents a fine equiaxial grain presenting a homogeneous dispersion of the precipitates in the solid solution with a well defined and regular onion rings, with a tail heading to the shoulder periphery, at the advancing side (detail "e" in Fig. 5). Fig. 5 shows a totally developed from top to bottom nugget, which means a weld seam with complete penetration. Moreover, it is not easily to distinguish any particles alignment at the root (detail "d" in Fig. 5), meaning a sound weld, which can very well represent the typical industrial situation of a fully developed FSW solution, with the right set of parameters. These results supports the developed algebraic model and prove that with the right set of parameters it is possible to eliminate some of the typical defects that may arise in FSW joints, namely voids in the advancing side (Fig. 2) and kissing bonds (Fig. 3) on the root which resulting from flawed stir of the materials during the processing, lack of penetration of the pin and insufficient vertical forging forces along the material thickness.

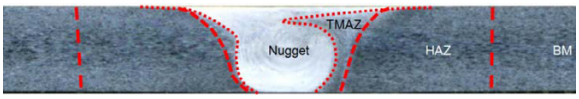

Fig. 11. Identification of the main different metallurgical zones on the FSW specimens in "as-welded" condition

4.2. Hardness results

Table 6 shows that welds conducted in higher travel speed present higher HARD's values. It is results of the decrease of energy available during the welding process that difficult the precipitates' dissolution and the dynamically recovering in nugget. From the results presented in Fig. 6 the following comments can be drawn: i) BM presents an average hardness of 163 HV05; ii) The hardness profiles at the three different penetration levels of the

weld seam cross section show in general a very small hardness drop from the base material characteristic value. The overall minimum value obtained was 130 HV05 at the middle level in the advancing side (interface between the TMAZ and the HAZ); iii) The average values obtained at the nugget is higher at the top level (160 HV05) and lower at the bottom level (145 HV05); iv) In general, the hardness values along the HAZ are lower at the middle level than at the top and bottom levels; v) The extension of the metallurgical modified zone by the FSW joint is about 28 mm in total (14 mm to each side of the joint).

4.3. Mechanical resistance results

Concerning the global analysis of the mechanical properties via the GETS and GEB coefficients, a reduction of 31% and 37% was achieved for the best of the nine conducted experiments, respectively. Overall, the FSW joints produced present more tensile than bending resistance. The results present in Table 11 validate the algebraic model since a reduction of 28.7% and 30.8%, was achieved, respectively, for GETS and GEB coefficients.

4.4. ANOVA results

Travel speed is the most significant parameter affecting both the GEB and HARD coefficients as given in Table 8 and 9, respectively. From Table 7, it can be seen that pin length is the most significant parameter for GETS.

4.5. Fatigue testing results

The equations obtained for the mean regression S-N lines for 50% probability of failure, (5) assuming N_r as the dependent variable and r^2 as the correlation coefficient, are given in Table 11. The gains in fatigue strain for $1x10^6$ cycles were also calculated.

$$N_r \Delta\sigma^m = K_0 \quad (5)$$

A decrease of the fatigue behaviour was obtained in the “as-welded” joints in comparison with the base material joints. The results (Table 11) show that the ground joints gave higher fatigue strengths in comparison with the base material joints. The grinding technique is especially better for lower loads and increases the high cycle fatigue strength. Progressively higher fatigue crack initiation periods were obtained in the ground joints, as reflected by the higher values of m in the equation of the S-N curve (Table 11). The gain in life is 1.42 for the ground joints without defects and 1.46 for the defective ones, considering 1x106 cycles.

Table 12. Equations of the mean fatigue S-N curves of Fig. 8

	m	K_0	r^2	*Gain in fatigue strength at $1x10^6$ cycles*
Base Material	4.053	$5.1x10^{14}$	0.9847	1.0
“As-welded” (non defective)	4.382	$2.3x10^{15}$	0.9674	(137/141)=0.97
Ground (non defective)	7.526	$2.1x10^{23}$	0.9849	(200/141)=1.42
“As-welded” (defective)	4.318	$9.8x10^{14}$	0.9105	(121/141)=0.86
Ground (defective)	8.064	$4.4x10^{24}$	0.9476	(206/141)=1.46

In Figures 9 and 10 cases the cracks propagated uniformly trough the specimen thickness. In both cases the crack initiate at top surface of the weld. In Fig. 9, multi-crack initiation is visible with the formation of large ductile type cracks with local tearing. The fracture is a mix of intergranular decohesion and transgranular cracking. Intergranular facets are visible, resulting from cleavage type fracture, which are highly faceted in nature. Hence, the surface roughness is considerably higher than in Fig. 10, obtained from the grinding technique. In both cases, the fracture process in zone II include transgranular mechanism, thus bands of fatigue striations can be seen. A secondary cracking mechanism is also noticeable in Fig. 9. In zone I, little formation of striation was observed, although slip bands appeared inside the grains, they were not enough to avoid separation from the grain boundaries.

5. Conclusions

The quality of FSW joints demonstrated to be very sensitive to the variation of the process parameters, mainly the travel speed and the pin's length. It is found that the parameter design of Taguchi method provides a simple, systematic, and efficient methodology for the optimization of the FS welding parameters. The implementation of FSW parameters predicted by the algebraic model resulted in sound complete penetration joints with a nugget zone developed over the total thickness with no perceptible root defect. The hardness values of the FSW sound joints are relatively homogeneous along the metallurgically modified zone having a minimum at the retreating side with an undermatch of about 18% relatively to base material. The global mechanical efficiency factors under static loading GETS and GEB reveal a decrease from the base material resistance properties more significant for the welded specimens under bending loading. An improvement in fatigue behaviour was obtained in the improved treated joints. The results show that the ground joints gave higher fatigue strengths in comparison with the base material and the "as-welded" joints. The weld grinding technique is especially better for lower loads and increases the high cycle fatigue strength. Progressively higher fatigue crack initiation periods were obtained in the ground joints.

Acknowledgements

The authors would like to acknowledge the technical support from the ESTS/Instituto Politécnico de Setúbal and the material supply by OGMA – Indústria Aeronáutica de Portugal S.A. a specialist aviation company since 1918.

References

[1] Focus Aluminium, *Revista Svetsaren*, Edited by ESAB, 2000, Vol.54 nº.2.

[2] Mendez P. F., New Trends in Welding in the Aeronautic Industry, *Proceedings of the conference New Trends for the Manufacturing in the Aeronautic Industry*, San Sebastian, Spain, May 24-25, pp.21-38, 2000.

[3] Vilaça, P., Quintino, L., Soldadura por Fricção Linear – O Que a Indústria Portuguesa Precisa e Precisa de Saber, *Tecnologia e Qualidade*, Revista do ISQ, nº 38, Abril/Junho de 2000, pp.46-57.

[4] Thomas, W., Nicholas, E., Kallee, S., Friction Based Technologies For Joining and Processing. Friction Stir Welding and Processing, *TMS Fall Meeting-Friction Stir Welding and Processing*, Indianapolis, USA, 2001, pp.3-13.

[5] Dawes, C., Thomas, W., Friction Stir Joining of Aluminium Alloys, *TWI Bulletin* 6, November/December 1995, pp.124-127.

[6] Dawes, C., Thomas, W., Friction Stir Process Welds Aluminium Alloys, *Welding Journal*, March, pp.41-45, 1996.

[7] Bhat, B., Carter, R., Ding, R., Lawless, K., Nunes, A., Russel, C., Shah, S., Friction-Stir Welding Development at NASA-Marshall Space Flight Center, *TMS Fall Meeting-Friction Stir Welding and Processing*, Indianapolis, USA, 2001, pp.117-128.

[8] Shepherd G.E., The Potential for using Solid Phase Welding to Repair Cracks that may occur on Thin Aluminium Aircraft Wing Structure, *2nd Internat. Symp. on FSW*, Gothenburg, Sweden, 2000.

[9] Mononen, J., Sirén, M., Hänninen, H., Cost Comparison of FSW and MIG Welded Aluminium Panels, *3rd International Symposium on Friction Stir Welding*, Port Island, Kobe, Japan, 2001.

[10]Vilaça, P., Fundamentos do Processo de Soldadura por Fricção Linear – Análise Experimental e Modelação Analítica, PhD Thesis, Instituto Superior Técnico, Universidade Técnica de Lisboa, Setembro 2003.

[11]Lomolino S., Tovo R., dos Santos J., D. Lohwasser, Fatigue strength of sound and defective friction stir welds on Al-Alloys for Airframes, *9th International Fatigue Congress*, Atlanta, USA, 14 to 19 May 2006.

[12]Lomolino S., Tovo R. and dos Santos J., On the fatigue behaviour and design curves of friction stir butt-welded Al alloys, *International Journal of Fatigue*, Volume 27, Issue 3, pp.305-316, March 2005.

[13]T. Santos, P. Vilaça and L. Quintino, Developments in NDT for Detecting Imperfections in Friction Stir Welds in Aluminium Alloys, *Welding in the World*, Volume 52, Nº 9/10, pp.30-37. 2008.

[14]Bowness, D., Lee, M.M.K., "Weld Toe Magnification Factors for Semi-elliptical Cracks in T-butt Joints – Comparation with Existing Solutions", International *Journal of Fatigue 2000*, **22**(5): 389-396, 2000.

[15]Newman, J.C., Raju, I.S., "Na empirical Stress-intensity Factor Equation for the Surface Crack". *Engineering Fracture Mechanics*, **15**(1/2):185-192, 1981.

[16]BS7910. "Guide on Methods for Assessing the Acceptability of Flaws in Structures", British Standards Institution, 1999.

[17]Raghunath, N., Pandey, Pulak M., Improving accuracy shrinkage modelling by using Taguchi method in selective laser sintering, *International Journal of Machine Tools & Manufacture*, Volume 47, pp.985-995, 2007.

[18]Nalbant, M., Gokkaya, H., Sur, G., Application of Taguchi method in the optimization of cutting parameters for surface roughness in turning, *Materials and Design*, Volume 28, pp.1379-1385, 2007.

[19]Bagchi, T.P., Taguchi Methods Explained, Prentice-Hall of India, 1993.